LOCATIONS OF ATMOSPHERIC PHOTOELECTRON ENERGY PEAKS WITHIN THE MARS ENVIRONMENT

R. A. FRAHM[1,*], J. R. SHARBER[1], J. D. WINNINGHAM[1], P. WURZ[2], M. W. LIEMOHN[3], E. KALLIO[4], M. YAMAUCHI[5], R. LUNDIN[5], S. BARABASH[5], A. J. COATES[6], D. R. LINDER[6], J. U. KOZYRA[3], M. HOLMSTRÖM[5], S. J. JEFFERS[1], H. ANDERSSON[5] and S. MCKENNA-LAWLER[7]

[1]*Southwest Research Institute, 6220 Culebra Road, San Antonio, TX 78228, USA*
[2]*University of Bern, Physikalisches Institut, Sidlerstrasse 5, CH-3012 Bern, Switzerland*
[3]*Space Physics Research Laboratory, University of Michigan, 2455 Hayward Street, Ann Arbor, MI 48105, USA*
[4]*Finnish Meteorological Institute, Box 503, FIN-00101 Helsinki, Finland*
[5]*Swedish Institute of Space Physics, Box 812, S-98 128, Kiruna, Sweden*
[6]*Mullard Space Science Laboratory, University College London, London RH5 6NT, UK*
[7]*Space Technology Ireland, National University of Ireland, Maynooth, Co. Kildare, Ireland*
*(*Author for correspondence: E-mail: frahm@swri.edu)*

(Received 2 February 2006; Accepted in final form 14 November 2006)

Abstract. By identifying peaks in the photoelectron spectrum produced by photoionization of CO_2 in the Martian atmosphere, we have conducted a pilot study to determine the locations of these photoelectrons in the space around Mars. The significant result of this study is that these photoelectrons populate a region around Mars bounded externally by the magnetic pileup boundary, and internally by the lowest altitude of our measurements ($\sim$250 km) on the dayside and by a cylinder of approximately the planetary radius on the nightside. It is particularly noteworthy that the photoelectrons on the nightside are observed from the terminator plane tailward to a distance of $\sim 3\ R_M$, the Mars Express apoapsis. The presence of the atmospherically generated photoelectrons on the nightside of Mars may be explained by direct magnetic field line connection between the nightside observation locations and the Martian dayside ionosphere. Thus the characteristic photoelectron peaks may be used as tracers of magnetic field lines for the study of the magnetic field configuration and particle transport in the Martian environment.

Keywords: Mars, photoelectrons

Introduction

On June 3, 2003, the European Space Agency (ESA) launched the Mars Express (MEX) spacecraft. The spacecraft reached Mars and was injected into orbit on December 25, 2003. One experiment on the MEX spacecraft is the Analyzer of Space Plasmas and Energetic Atoms-3 (ASPERA-3) (Barabash *et al.*, 2004), which measures *in situ* ions, electrons, and energetic neutral atoms at Mars. Ambient electrons are measured *in situ* by the Electron Spectrometer (ELS) of ASPERA-3.

Space Science Reviews (2006) 126: 389–402
DOI: 10.1007/s11214-006-9119-5
© Springer 2007

source: https://doi.org/10.48350/20783 | downloaded: 12.10.2024

Prior to the launch of Mars Express, it was known that the Mars ionospheric electron spectrum contained photoelectron peaks resulting from the photoionization of atmospheric gases. Based on neutral mass spectrometer data obtained from the Mars Viking lander and a solar spectrum (Hinteregger, 1976), Mantas and Hanson (1979) calculated the electron spectrum below 100 eV in the Mars atmosphere, with both horizontal and vertical magnetic fields, demonstrating the presence of spectral peaks in the range of 21–24 eV and at 27 eV. These results were corroborated later that same year by a model of Fox and Dalgarno (1979) without a magnetic field, and later updated by Fox (2004). These electron peaks result primarily from the ionization of CO_2 by solar He 30.4 nm photons produced for the most part in the photochemical equilibrium region and transported to higher altitudes. Thus the photoelectron peaks detected at a remote location may be considered as tracers of the magnetic field line to the production region (Frahm *et al.*, 2006). Evidence of these peaks was observed in the spectral measurements of the Electron Reflectometer (ER) on Mars Global Surveyor (MGS) (Mitchell *et al.*, 2001), but they were not resolved by that instrument. The peaks were first resolved by spectral measurement with the electron spectrometer on Mars Express (Lundin *et al.*, 2004; Frahm *et al.*, 2006), which began routine operations in its orbit around Mars in early 2004.

The paper reporting the photoelectron peaks in the Martian ionosphere (Frahm *et al.*, 2006) described the early results from ELS, demonstrating the presence of the photoelectron peaks and their relationship to the sheath of shocked solar wind plasma. In that paper it was pointed out that the CO_2 photoelectron peaks are routinely observed on the dayside of the planet at and above the MEX periapsis altitude of ~250 km. The peaks were also reported on the night side of the terminator plane, sometimes very distant from Mars, even near apoapsis, at more than 10,000 km altitude. (During 2004 the MEX apoapsis changed from an altitude of ~11,600 km to ~10,100 km and periapsis changed from an altitude of ~270 km to ~250 km in mid year to ~300 km at the end of the year.) In an effort to understand how these photoelectrons reach the large distances, Liemohn *et al.* (2006) used ELS photoelectron observations and simulations with a global MHD code (Ma *et al.*, 2002, 2004) to study the likely paths of the electrons detected by the spacecraft. Two of the three cases studied indicated that the photoelectrons were produced on open field lines connecting to the planet in the afternoon/evening sector, while the third suggested that the photoelectrons were observed on interplanetary field lines draping the planet.

Based on the notion that photoelectrons may be used as tracers of the magnetic field configuration near Mars, we expand on our previous work by making use of the large body of observations obtained from the MEX electron spectrometer to determine the location of the CO_2 photoelectrons in the space around the planet. We report here the results of this pilot study, which used electron data for most of the year 2004. In some ways the results are quite surprising, in that a large number of photoelectrons were found far down the Martian tail and generally outside the umbral region. These findings provide clues about the magnetic field configuration

and the transport of photoelectrons in the Martian environment. They may also be compared with simulations using global scale MHD modeling (see Liemohn *et al.*, this issue).

Instrument

The ELS is a spherical top-hat analyzer with a field of view of $360^\circ \times 4^\circ$. The 360° measurement plane is divided into 16 sectors, each sector is 22.5° wide. The ELS analyzer constant (the average value is 7.23 ± 0.05 eV/volt) and energy resolution (average value of $\Delta E/E = 0.083 \pm 0.003$) are slightly sector dependent and were determined by laboratory measurements at 10 keV. Measurements of variations in the analyzer constant and energy resolution as functions of energy indicated an energy-dependent, relative efficiency factor for each sector. Sector comparisons using a stable nickel-63 nuclear source determined these energy-dependent variations. The energy independent physical geometric factor was determined to be 5.88×10^{-4} cm^2 sr from simulation.

The ELS covers the energy range from 0.4 eV to 20 keV with a dual range deflection power supply. The deflection voltage ranges from 0 to 20.99 V for the low range and 0 to 2800.0 V for the high range. The energies selected are sector dependent, but have maximum values of approximately 150 eV and 20 keV. Each supply has a control resolution of 4096 linear voltage values within its full range. Of the 8192 possible deflection voltage values, 128 are selected to comprise the ELS energy sweep. The values are sequenced from highest to lowest voltage in a time of 4 s. The last sweep step is a fly-back step and is ignored in the data analysis.

Most of the ELS data examined in this paper were acquired under normal energy resolution and high time resolution; however, some of the data were acquired in high energy resolution and high time resolution modes. In a few cases, data were used when ELS was in its low energy resolution and low time resolution modes. *High energy resolution* means that data are acquired with energy steps less than the energy bandwidth (ΔE) of the analyzer, and the spectral values of each sweep are telemetered; at *normal energy resolution*, data are acquired with energy steps equal to the energy bandwidth (ΔE), and spectral values of each sweep are telemetered. In *low energy resolution* mode, data are acquired at energy steps equal to the energy bandwidth (ΔE), but the spectral measurement is degraded by addition of spectral values over 2, 4, or 8 energy steps before being telemetered. In *high time resolution*, a complete ELS energy sweep occurs within 4 s and is fully telemetered. *Lower time resolution* modes are degraded by addition of full energy sweeps (2, 4, 8, or 16 sweeps) before being telemetered.

The ELS instrument is mounted on the ASPERA-3 scan platform, which makes possible full 3D electron distributions. However, this platform was not activated until January of 2006 and its use has been limited since. Only ELS data from 2004 have been used in the pilot study.

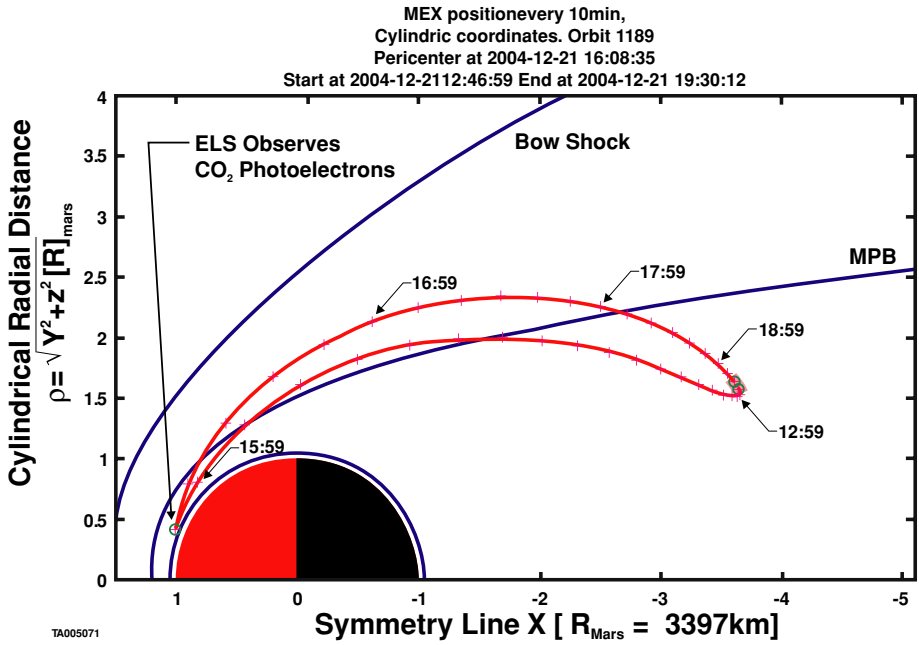

Figure 1. Mars Express orbit 1189 on December 21, 2004. As Mars Express traveled through the dayside ionosphere, photoelectron peaks were observed. Mars cylindrical coordinates with the Sun at the left, are used to express the spacecraft orbit as distance from the Mars-Sun line. The blue curves mark the average positions of the bow shock and MPB (Magnetic Pileup Boundary) as derived by Vignes *et al*. (2000).

Observations

A measurement of the photoelectrons in the Martian ionosphere on December 21, 2004 is illustrated in Figures 1, 2, and 3. Figure 1 describes the location of the MEX orbit in cylindrical coordinates, ρ and X of the Mars-centered Solar Orbital (MSO) system (unabberated). In the MSO system, X points toward the Sun, Z is perpendicular to the planet's velocity and is directed toward the northern ecliptic hemisphere, and Y completes a right handed, orthogonal system. The coordinate $\rho = \sqrt{Y^2 + Z^2}$. In Figure 1 the Sun is to the left, and the outer blue curves mark the average positions of the bow shock and magnetic pileup boundary (MPB) as determined by Vignes (2000) based on 290 orbits of MGS observations. The innermost blue circle marks 150 km altitude.

Measurements of ELS electrons in the minutes before and after periapsis on Day 356 of 2004 are shown in Figure 2. The plots are energy-time spectrograms of 17 minutes of data beginning at 1600:00 UT of Day 356 with periapsis at 1608:24 UT. Figure 2 shows measurements from four directions looking from the spacecraft: toward Mars, away from Mars, toward the East, and toward the West. Two enhancements of electron energy flux occurring at energies near 20 eV are observed

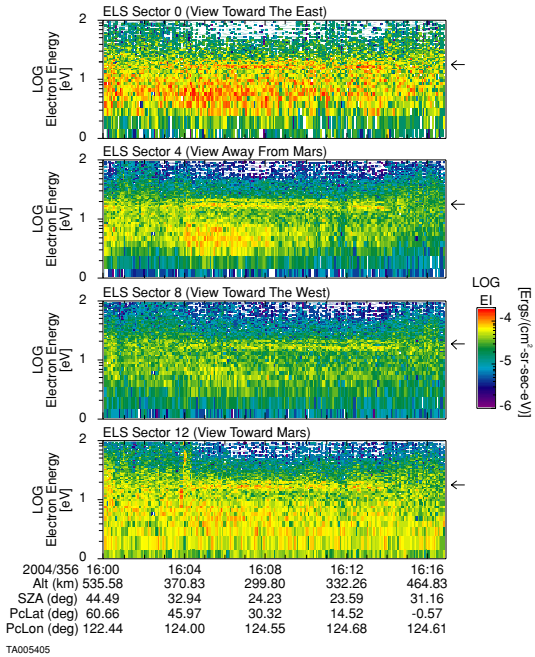

Figure 2. Energy-time spectrogram in the Martian ionosphere. Values of differential energy intensity are color coded. Spectrograms are marked in terms of view from the spacecraft and show photoelectron peaks measured in selected directions. Spacecraft location is given in terms of planetodetic altitude (Alt), solar zenith angle at the spacecraft (SZA), planetocentric latitude (PcLat), and planetocentric longitude (PCLon), which is measured toward the east. An arrow at the right of each spectrogram marks the approximate energy of the photoelectron peaks.

in each spectrogram between about 1604 and 1614 UT (their approximate energy is marked at the right of each panel with an arrow). They are not quite so easy to see in the first plot (toward East) because of higher fluxes below 20 eV. These enhancements are the major peaks in the photoelectron spectrum resulting from ionization of CO_2 in the Mars atmosphere. They are a unique signature of photoionization. On this pass they are measured from an altitude of 370 km on the inbound part of the orbit, through periapsis (300 km altitude), and out to 412 km on the outbound portion.

Further examination of the photoelectron spectra near periapsis is presented in Figure 3, which shows photoelectrons directed (a) away from Mars and (b) toward Mars. The spectra are plotted as energy intensity in units of ergs/(cm^2 s sr eV) and were obtained by averaging over a two-minute interval centered near periapsis. Also shown are the measurement uncertainties at the $+$ and -1σ level, which include Poisson counting statistics, errors resulting from the telemetry compression scheme, and instrumental uncertainties. The spectra show the signature of the photoelectron peaks at about 21 eV and about 17 eV. The theoretical locations of these

peaks are 27 eV and 21–24 eV, which indicates that during this time, the spacecraft was charged to about −6 volts. It is important to note that these photoelectron features in the electron energy spectrum, although shifted in energy, are easily recognizable, because the electrons have been produced uniquely and in sufficient numbers for easy identification. Our ability to distinguish these atmospherically produced photoelectrons from those produced by the spacecraft is based on this identification of the peaks characteristic of the Mars atmospheric environment, as discussed earlier. These usually stand out easily even when spacecraft-produced photoelectrons and secondary electrons are present. Further information may be found in Frahm *et al*. (2006).

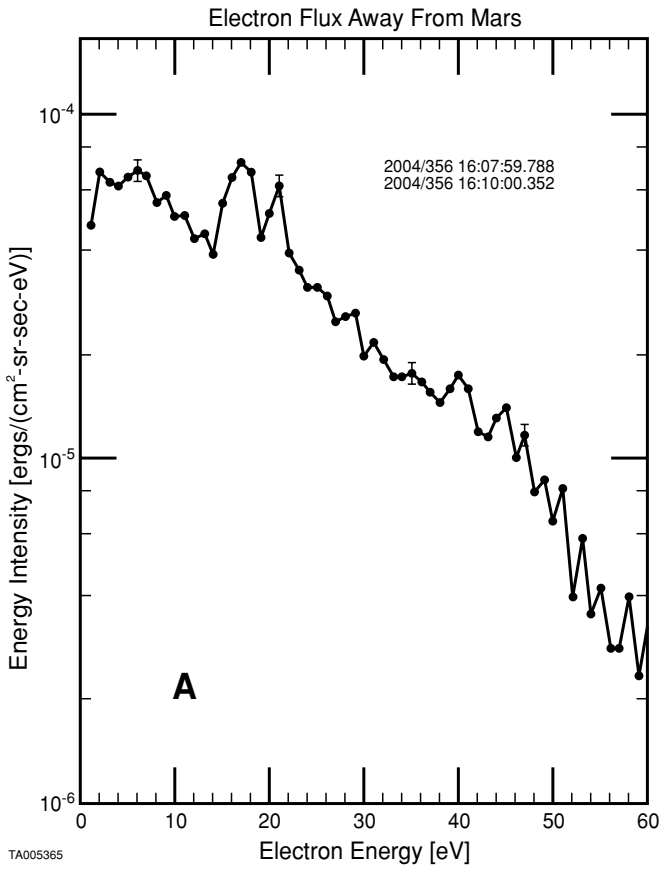

Figure 3. Electron spectra at periapsis. Shown in (a) is the spectrum of electrons flux away from Mars and in (b) is the spectrum of electrons flux toward Mars. These data are taken near periapsis as a 2 minute average. Each energy spectrum is shown as energy intensity. Error bars include Poisson statistics, telemetry compression errors, and instrument uncertainties.

(*Continued on next page*)

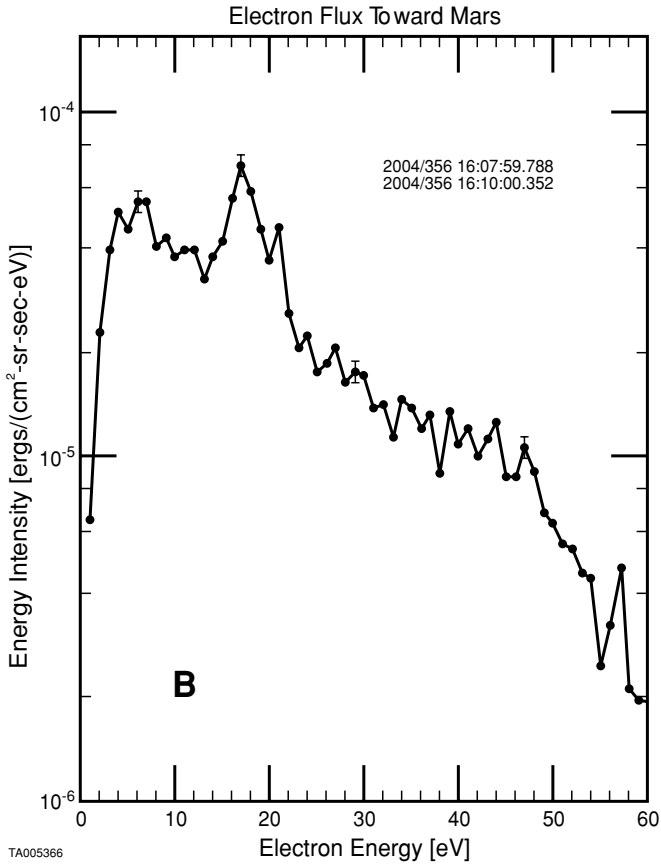

Figure 3. (*Continued*)

In the ELS data we see photoelectron peaks at essentially all altitudes sampled by the Mars Express orbit. Figure 4 shows eleven spectra measured at various altitudes over this range. The energy range of the photoelectron peaks in each spectrum is highlighted. There is some variation in the magnitudes of the signature peaks from one spectrum to another, but all are comparable. This has bearing on the source region and will be discussed later. The spectrum measured at the lowest altitude was obtained in the ionosphere near periapsis (260 km) in the sunlit atmosphere. The spectrum measured at the highest altitude was obtained near apoapsis where the spacecraft altitude was 10,100 km. In Table I we provide the date and time of each spectral measurement shown in Figure 4, along with altitude, planetodetic latitude and longitude, solar zenith angle, and local solar time of each observation. The ranges of each entry correspond to the beginning and end time of each spectral measurement. The table entries are arranged in order of increasing altitude.

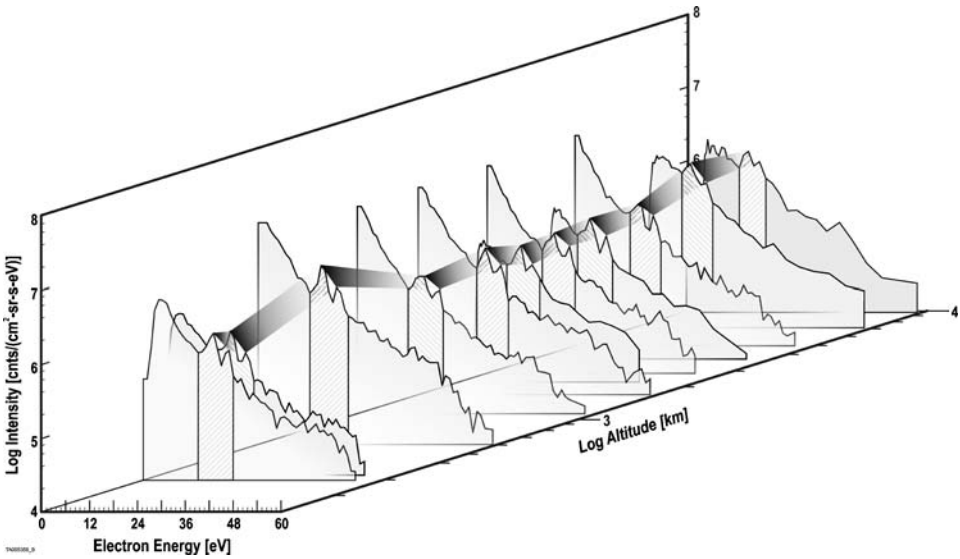

Figure 4. Electron spectra obtained at periapsis and apoapsis and selected altitudes in between, illustrating that the atmospheric photoelectron peaks can be found over the entire altitude range of the spacecraft. Energy bands containing the atmospheric photoelectron peaks are highlighted.

TABLE I

Orbit-altitude data for photoelectron spectra of Figure 4.

Year	Day	Universal Time (hh:mm:ss)	Altitude (km)	PD Latitude (deg)	PD Longitude (deg)	Solar Zenith Angle (deg)	Solar Time (hr)
2004	176	22:07:29–22:09:44	267.6–295.7	−86.56–−81.10	296.45–10.46	112.56–107.26	2.15–3.76
2004	156	04:46:27–04:47:35	299.1–327.9	−67.57–−63.03	98.23–99.51	92.21–88.68	5.75–6.09
2004	107	10:45:56–10:50:34	628.9–385.5	−85.69–−75.49	168.07–281.66	102.1–86.02	4.93–7.20
2004	187	19:56:38–19:57:46	1206.9–1109.2	−14.81–−17.86	345.57–345.49	123.37–124.18	20.33–20.42
2004	187	19:51:00–19:52:09	1696.0–1604.4	−02.05–−04.18	346.13–346.02	118.48–119.55	19.88–19.94
2004	178	00:30:01–00:33:24	2222.2–1908.7	+2.48–−3.58	187.54–187.09	121.42–124.12	20.11–20.28
2004	178	07:06:33–07:07:38	2863.7–2769.9	+13.15–+11.75	90.26–90.10	115.8–116.58	19.74–19.79
2004	172	03:04:59–03:07:14	3698.8–3488.6	+20.35–+17.77	94.49–94.10	114.71–116.24	19.18–19.79
2004	166	19:08:57–19:10:06	4832.6–4738.0	+29.26–+28.32	164.69–164.48	111.49–112.19	19.56–19.62
2004	115	07:00:01–07:03:04	7107.4–6900.8	+13.20–+11.68	242.65–242.02	147.11–148.08	21.91–21.95
2005	009	13:43:26–13:44:32	10113.3–10113.4	−40.34–−39.99	150.51–150.26	153.05–153.33	23.98–23.99

To determine the occurrence and locations of the CO_2 photoelectrons in an aggregate sense in the space around Mars, we conducted a pilot statistical study using ELS data taken between January 5 and November 13 of 2004. For simplicity only one ELS sector (sector 3) was used, and consequently, for this study, the statistics do not register the flow direction at each location. Statistics were built up by accumulating the occurrence and location in MSO coordinates of every spectrum containing the CO_2 photoelectron peaks. For two-dimensional presentations, the data are then binned into 100×100 km bins in that system.

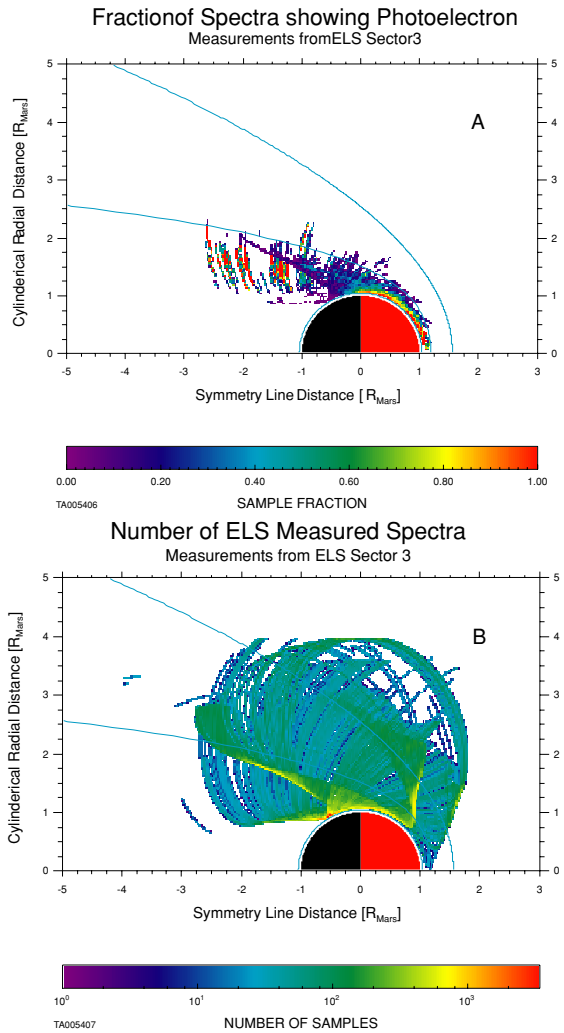

Figure 5. Fractional occurrence of atmospheric photoelectron peaks. The region near Mars is examined to show (a) the fraction of occurrence of atmospheric photoelectrons peaks and (b) number of samples made by the ELS. In both cases, the sun is at the right, and the average positions of the Martian bow shock and MPB, as determined by Vignes *et al*. (2000), are shown. Note that a zero-sample fraction is shown as the background color (see text).

The results of the study are presented in Figure 5. In Figure 5(a) each pixel of data represents a fractional occurrence of the CO_2 photoelectron peaks, color-coded by the scale below the plot. Figure 5(b) shows the regions sampled by Mars Express at times when ELS was on. Also shown in Figure 5(a) are the average positions of the bow shock and MPB as determined by Vignes *et al*. (2000) using MGS magnetometer and electron observations. It is clear from Figure 5a that most of the photoelectron signatures are found within the average MPB. In other words,

the atmospherically produced photoelectrons, whether they were detected near or far from the planet, were inside the magnetic pileup region. We have checked the points outside the MPB curve of Figure 5a (an average); and, using ELS data, all of these lie below the altitude range over which the shocked solar wind electrons are absorbed. This region defines the MPB (Crider *et al.*, 2000; Vignes *et al.*, 2000); thus every point in the figure definitely lies within (below) the instantaneous magnetic pileup boundary. We note here that in the presentation of Figure 5(a), there is no distinction made between a "zero" that results because the region was not sampled and a "zero" that results when the region is sampled and no photoelectron peaks are observed. These may be distinguished with the help of Figure 5(b), which shows the regions sampled.

In Figure 5 one also observes that the frequency of occurrence of photoelectron peaks is largest on the dayside of the planet at low altitudes in the ionosphere. This is consistent with their copious production in the photochemical equilibrium layer below. We also note that the atmospheric photoelectron peaks were not seen in the solar wind; i.e., they are not seen anywhere near or outside of the statistical bow shock in spite of good sampling of the interplanetary medium.

Figures 6 and 7 show the same data (shown in Figure 5) in different perspectives. Figure 6 shows the data from the dayside of Mars ($X > 0$) projected onto the *YZ*-plane, while Figure 7 shows data from the night side ($X < 0$) projected onto the same plane. These figures show where the ELS measurements were obtained and also where the sampling was incomplete (shown in the (b) part of each figure). The dayside data (Figure 6) indicates good coverage at locations away from the planet,

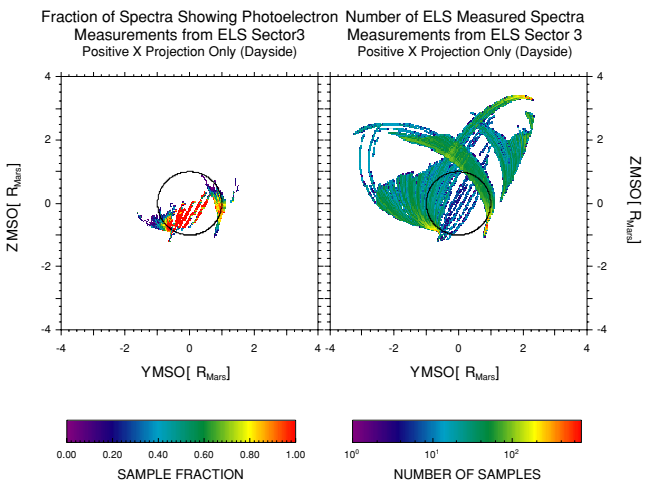

Figure 6. Dayside ELS measurements. The data of Figure 5 for $X > 0$ are projected on the *YZ*-plane. The fraction of times photoelectrons measured are shown in (a), while the total number of measurement points is shown in (b). Note that a zero-sample fraction is shown as the background color (see text).

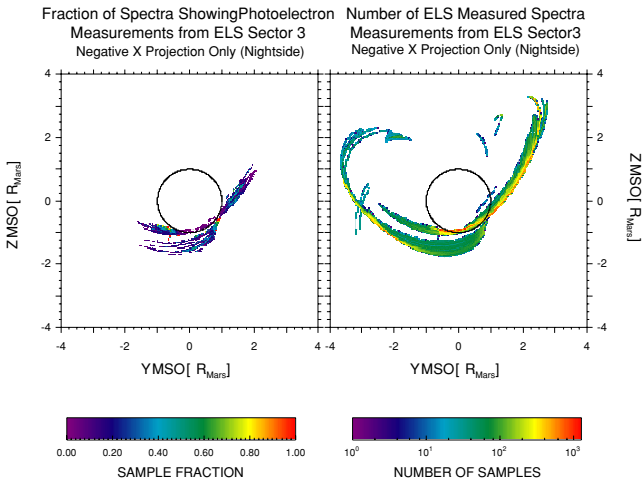

Figure 7. Nightside ELS measurements. The data of Figure 5 for $X < 0$ are projected on the *YZ*-plane. The fraction of times photoelectrons are measured are shown in (a) while the total number of measurement points is shown in (b). Note that a zero-sample fraction is shown as the background color (see text).

but the small number of measurements occurs at altitudes too high for detection of the photoelectron peaks. In Figure 7, the gap just below the outline of the planet in Figure 7(a) results from the similar sampling gap in Figure 7(b) indicating that there is no coverage at that location.

Usually when MEX is far from Mars, the measurement plane of ELS is parallel to the Mars orbital plane. As the spacecraft nears the planet, MEX is generally commanded into one of two observational modes. The first keeps the ELS measurement plane parallel to the Mars orbital plane (one sensor will look along the Mars-Sun line), and the second tilts the spacecraft such that the planet radial vector is parallel to the ELS measurement plane. Since this pilot study uses only one ELS sector (sector 3), it is possible that the difference in aspect resulting from different spacecraft observational modes might affect our statistics. It has been demonstrated that the measurement of flows can be very aspect sensitive at large distances from the planet (Frahm *et al.*, 2006; Liemohn *et al.*, 2006). The slightly reduced occurrence percentages in the region near $-0.75\ R_M < X < -0.25\ R_M$ of Figure 5 could be an indication of this, as this is the region where MEX often maneuvers into the ELS radial measurement configuration. At this point this effect is a possibility and will be investigated further in future work.

Discussion

The significant result of this study is that atmospherically produced photoelectrons populate a region around Mars bounded externally by the magnetic pileup boundary,

and internally by the lowest altitude of our measurements (~250 km) on the dayside and by the a cylinder defined approximately by the edge of the planet's shadow on the nightside. On the nightside, the photoelectrons were observed as far from the terminator plane as ~3 R_M. The dayside results may be understood in terms of ionization of atmospheric carbon dioxide (with some ionization of atomic oxygen) by solar extreme ultraviolet radiation (Frahm *et al.*, 2006, and references therein). However, it is the observation of the CO_2 photoelectrons at large distances down the flanks of the magnetosheath that is the unexpected result of this study. How then might atmospherically generated photoelectrons be found at such distances?

The fact that the CO_2 peaks measured in the distant locations have magnitudes comparable to those measured on the dayside argues strongly for a direct connection, most likely along magnetic field lines, to the production region – in this situation the dayside ionosphere. Both observations and simulation studies suggest such a connection.

The solar wind interaction with Mars results in a "draping" magnetic field morphology (Nagy *et al.*, 2004). Measurements using the Magnetometer/Electron Reflectometer on Mars Global Surveyor (Bertucci *et al.*, 2005) have shown the draping effect to be easily measured within the magnetic pileup *region* (MPR), the region immediately interior to the MPB. Typically, as MGS moves from the shocked solar wind (magnetosheath), through the MPB and into the MPR, the magnetic field continues to pile up (strengthens), became more regular (contains progressively fewer fluctuations), and exhibits the draping quality. Draping is not detected within the shocked solar wind. The lower boundary of the MPR is within the ionosphere and may be as low as the exobase (Mitchell *et al.*, 2001; Nagy *et al.*, 2004). Based on our own observations (e.g., Figure 2), this is the region we know to be a source region for the CO_2 photoelectrons on the dayside of Mars. Thus the MGS observations place the dayside photoelectron source on draped field lines, some of which have a high likelihood of connecting with down-tail regions shown by this study to be populated by the photoelectrons.

Simulations have provided another means to study the particle and field environment. For example, Ma *et al.* (2004), using an MHD model run for maximum solar wind conditions and the presence of crustal fields, show a magnetic pileup region, draping of the magnetic field, and minimagnetospheres resulting from the presence of relatively strong crustal magnetic field sources (Harnett and Winglee, 2003). In the Ma *et al.* (2004) simulations, some field lines emanating from crustal source regions connect the dayside ionosphere to nightside locations.

In a study reported in this issue, Liemohn *et al.* (this issue) have used the Ma *et al.* (2004) code to look specifically at the question of magnetic field line connectivity between the dayside ionosphere and regions antisunward of the terminator plane. In the simulation, magnetic field lines were extracted from an array of starting points in the terminator plane connecting the dayside and nightside regions. As a part of the study, statistics were recorded on the fraction of field lines showing magnetic connectivity to the dayside ionosphere. This enabled a very direct comparison

with the results of our study. The Liemohn *et al.* (this issue) results are strikingly similar to the ELS statistics shown in our Figure 5, making clear the connection between the dayside ionosphere and locations antisunward of the terminator plane, including the photoelectrons observed several R_M tailward of that plane. Liemohn *et al.* conclude that "the high-altitude photoelectrons are the result of direct magnetic connectivity to the dayside at the moment of the measurement, and no extra trapping or bouncing mechanisms are needed to explain the data." We completely agree with that conclusion.

Since atmospheric photoelectrons, originating from the dayside, are observed in the tail of Mars, by charge conservation there must also be low energy planetary ions at those locations. A study of the relation between low-energy planetary ions and photoelectrons will be a natural follow-on to this study. Low-energy planetary ions are confirmed to be observed with the photoelectrons at more than 10,000 km (the pass of the last entry in Table I).

Conclusions

By identifying peaks in the photoelectron spectrum produced by photoionization of CO_2, we have conducted a pilot study to determine the locations of these photoelectrons in the space around Mars.

The significant result of this study is that these photoelectrons populate a region around Mars bounded externally by the magnetic pileup boundary, and internally by the lowest altitude of our measurements ($\sim$250 km) on the dayside and by a cylinder of approximately the planetary radius on the nightside. It is particularly noteworthy that the photoelectrons on the nightside are observed from the terminator plane tailward out to a distance of $\sim 3\ R_M$, the MEX apoapsis.

The presence of the atmospherically generated photoelectrons on the nightside of Mars may be explained by direct magnetic field line connection between the nightside observation locations and the Martian dayside ionosphere. Thus the characteristic photoelectron peaks may be used as tracers of magnetic field lines for the study of the magnetic field configuration and particle transport in the Martian environment.

Acknowledgements

The ASPERA-3 experiment on the European Space Agency (ESA) Mars Express mission is a joint effort between 15 laboratories in 10 countries, all sponsored by their national agencies. We thank all these agencies as well as the various departments/institutes hosting these efforts. We wish to acknowledge support through the National Aeronautics and Space Administration (NASA) contract NASW-00003 in the United States, Particle Physics and Astronomy Research Council (PPARC) in the United Kingdom, and wish to thank those NASA officials who had the foresight to allow augmentation of the original ASPERA-3 proposal for ELS so that

it would provide the additional capabilities which allowed the science described in this paper to be conducted. We also wish to acknowledge the Swedish National Space Board for their support of the main PI-institute and we are indebted to ESA for their courage in embarking on the Mars Express program, the first ESA mission to the red planet.

References

Barabash, S., *et al.*: 2004, in Wilson, A., and Chicarro, A. (eds.), *Mars Express: The Scientific Payload*, European Space Agency Special Report SP-1240, European Space Agency Research and Scientific Support, European Space Research and Technology Centre, Noordwijk, The Netherlands, p. 121.

Bertucci, C., Mazelle, C., and Acuña, M. H.: 2005, *J. Atmos. Sol. Terr. Phys.* **67**, 1797.

Crider, D., Cloutier, P., Law, C., Walker, P., Chen, Y., Acuña, M., *et al.*: 2000, *Geophys. Res. Lett.* **27**(1), 45.

Fox, J. L.: 2004, *J. Geophys. Res.* **109**, A11310, doi:10.1029/2004JA010380.

Fox, J. L., and Dalgarno, A.: 1979, *J. Geophys. Res.* **84**, 7315.

Frahm R., *et al.*: 2006, *Icarus* **182**, 371.

Harnett, E. M., and Winglee, R. M.: 2003, *Geophys. Res. Lett.* **30**(20), 2074, doi:10.1029/2003GL017852.

Hinterreger, H. E.: 1976, *J. Atmos. Terr. Phys.* **38**, 791.

Liemohn, M. W., *et al.*: 2006, *Icarus* **182**, 383.

Liemohn, M. W., Ma, Y., Frahm, R. A., Fang, X., Kozyra, J. U., Nagy, A. F., *et al.*: *Space Sci. Rev.*, this issue, doi: 10.1007/s11214-006-9116-8.

Lundin, R., *et al.*: 2004, *Science* **305**, 1933.

Ma, Y., Nagy, A. F., Hansen, K. C., DeZeeuw, D. L., Gombosi, T. I., and Powell, K. G.: 2002, *J. Geophys. Res.* **107**(A10), 1282, doi:10.1029/2002JA009293.

Ma, Y., Nagy, A. F., Sokolov, I. V., and Hansen, K. C.: 2004, *J. Geophys. Res.* **109**, A07211, doi:10.1029/2003JA010367.

Mantas, G. P., and Hanson, W. B.: 1979, *J. Geophys. Res.* **84**, 369.

Mitchell, D. L., Lin, R. P., Mazelle, C., Réme, H., Cloutier, P. A., Connerney, J. E. P., *et al.*: 2001, *J. Geophys. Res.* **106**, 23419.

Nagy, A. F., *et al.*: 2004, *Space Sci. Rev.* **111**, 33.

Vignes, D., Mazelle, C., Réme, H., Acuña, M. H., Connerney, J. E. P., Lin, R. P., *et al.*: 2000, *Geophys. Res. Lett.* **27**, 49.